Canadian Mineralogist
Vol. 28, pp. 67-75 (1990)

HALOGEN-BEARING ALLANITE FROM THE WHITE RIVER GOLD OCCURRENCE, HEMLO AREA, ONTARIO

YUANMING PAN AND MICHAEL E. FLEET

Department of Geology, University of Western Ontario, London, Ontario N6A 5B7

ABSTRACT

Halogen-bearing allanite (containing up to 0.95 wt.% Cl and 0.76 wt.% F) occurs as a minor constituent in the zone of anomalous gold values at the White River gold occurrence of LAC Minerals Ltd., Hemlo area, Ontario. It is present as fine-grained aggregates associated with monazite, apatite, rutile, zircon, clinozoisite, and epidote and exhibits a well-developed chemical zonation with an Fe- and *REE*-poor core and an Fe- and *REE*-rich margin. *REE*-bearing and *REE*-free clinozoisite also are locally present as nuclei to the *REE*-poor core. Halogen-bearing allanite has minor Mg and Mn and an extremely low content of ferric iron. Clinozoisite and halogen-bearing allanite exhibit a complete solid-solution through the coupled substitution: Ca_{A2} + Al_{M3} = REE_{A2} + $Fe^{2+}{}_{M3}$. Textures and chemical composition indicate that the halogen-bearing (F, Cl) allanite from the study area crystallized from a H_2O-rich fluid during the formation of the calc-silicate (skarn) assemblage. Hydrothermal fluid, probably directly or indirectly related to plutonic activity, introduced F and Cl and remobilized and locally concentrated *REE*. The restricted occurrence of halogen-bearing allanite and its close correlation with high gold concentrations in the Anomalous Zone support a genetic link between calc-silicate alteration and gold mineralization in this Archean terrain, analogous to that in Phanerozoic auriferous skarn deposits.

Keywords: F- and Cl-bearing allanite, gold mineralization, local remobilization of *REE*, calc-silicate (skarn) alteration, Hemlo area, Ontario.

SOMMAIRE

Nous avons découvert une allanite enrichie en halogènes (jusqu'à 0.95% en poids de Cl et 0.76% de F) comme accessoire dans une zone aurifère de l'indice de White River, propriété de la société LAC Minerals, dans le camp minier de Hemlo, en Ontario. L'allanite forme des agrégats avec monazite, apatite, rutile, zircon, clinozoïsite et épidote; les cristaux, qui sont bien zonés, montrent un coeur à faible teneur en Fe et en terres rares (*TR*), et une bordure enrichie dans ces éléments. La clinozoïsite, avec ou sans terres rares, forme le nucléus de tels cristaux dans certains cas. L'allanite contient de faibles quantités de Mg et de Mn, et une très faible teneur en Fe^{3+}. Clinozoïsite et allanite enrichie en halogènes définissent une solution solide complète selon la substitution couplée Ca_{A2} + Al_{M3} = TR_{A2} + $Fe^{2+}{}_{M3}$. La texture et la composition chimique font penser que cette allanite a cristallisé à partir d'une phase fluide aqueuse au cours de la formation des assemblages de calc-silicates (skarns). La phase fluide, probablement dérivée directement ou indirectement d'une activité plutonique, a introduit le fluor et le chlore, et a remobilisé et localement concentré les terres rares. La distribution restreinte de l'allanite et sa corrélation étroite avec les endroits enrichis en or dans la zone dite "anomale" seraient l'expression d'un lien génétique entre la formation des calc-silicates et la minéralisation en or dans ce socle archéen, tout comme dans les gisements aurifères des skarns d'âge phanérozoïque.

(Traduit par la Rédaction)

Mots-clés: allanite enrichie en F et Cl, minéralisation aurifère, mobilisation locale des terres rares, formation des calc-silicates (skarns), région de Hemlo, Ontario.

INTRODUCTION

Allanite is an epidote-group mineral with the general formula $A_2M_3Si_3O_{12}(OH)$. The ten-fold-coordinated $A(1)$ site is always fully occupied by Ca; the large cations, such as the *REE* and possibly Mn^{2+}, which may substitute for Ca, partly occupy the nine-fold-coordinated $A(2)$ site. Ferrous iron, along with Fe^{3+}, Mn^{3+}, Mn^{2+}, Mg and Ti, is present in the relatively large $M(3)$ site (Dollase 1971). The ideal end-member composition for allanite, then, may be represented as $Ca(REE)Fe^{2+}Al_2Si_3O_{12}(OH)$. Allanite compositions reported to date represent a solid solution with the $FeAl_2$-epidote end-member species through the coupled substitution: Ca_{A2} + Fe^{3+}_{M3} = REE_{A2} + Fe^{2+}_{M3}. Allanite is a characteristic accessory mineral in many granites, granodiorites, monzonites, syenites, and pegmatites (Deer *et al.* 1986 and references herein), and also is a common mineral in limestone skarns (Geijer 1927, 1961, Papunen & Lindsjö 1972) and hydrothermal veins (Bromley 1964, Exley 1980).

Although allanite occurs in a wide variety of rock types and exhibits a wide variation in chemical composition, varieties with volatile anion species other than $(OH)^-$ are considered to be rare (Deer *et al.* 1986). Fluorine-bearing allanite has been reported at the contact between calc-granulite and microcline pegmatite from India (Rao *et al.* 1979) and in quartz veins in granites of the Itulin tin–tungsten deposit from the USSR (Ivanov *et al.* 1981). The present paper reports on a halogen-bearing (F, Cl) variety of allanite in a calc-silicate (skarn) assemblage associated with a gold occurrence from the Hemlo area, Ontario.

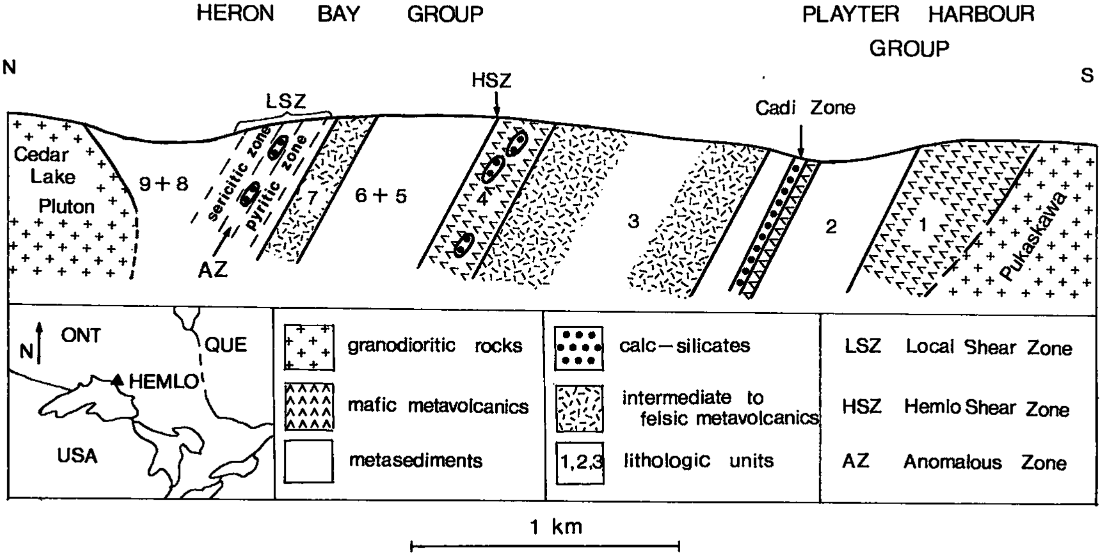

FIG. 1. Schematic cross-section of the Hemlo - Heron Bay greenstone belt at the White River gold occurrence, Hemlo area, Ontario (lateral extent of calc-silicate occurrences in Cadi Zone, Unit 4 and Anomalous Zone is exaggerated).

GEOLOGY OF THE WHITE RIVER GOLD PROSPECT

The White River gold occurrence of LAC Minerals Ltd. is located about 5 km east along the strike of the Hemlo gold deposit within the Hemlo - Heron Bay Archean greenstone belt of the Wawa Subprovince of the Superior Province (Pan & Fleet 1988). The supracrustal rocks, which strike 95–110° and dip 60° to the north, are subdivided into two groups: the Playter Harbour Group to the south and the Heron Bay Group to the north (Muir 1982), and are underlain by crystalline basement (the Pukaskwa Gneissic Complex) to the south and a late granodioritic intrusive body (the Cedar Lake Pluton) to the north (Fig. 1). Polymetamorphism related to heterogeneous shear deformation is characterized by a low-pressure peak metamorphism that climaxed in two narrow structural zones at middle amphibolite facies within lithologic unit 1, along the contact with the Pukaskwa Gneissic Complex, and within lithologic units 4, 5, and 6, enclosing the regional Hemlo Shear Zone (Fig. 1); over the rest of the study area, the peak metamorphism was generally at greenschist–amphibolite transitional facies (Pan & Fleet 1988, 1989a). A regional, calc-silicate-like (skarn) alteration overprinted all supracrustal rocks after the peak of metamorphism, particularly along structural failures of the greenstone belt. In the northern part of the study area (Fig. 1), a narrow but continuous zone of anomalous gold values (Anomalous Zone) occurs, in proximity to the Cedar Lake Pluton, within a local brittle–ductile shear zone at or near lithologic boundaries between underlying intermediate to felsic metavolcanic rocks (unit 7) and overlying metapelites (unit 8) (Pan & Fleet 1989a). Maximum gold values (up to 27 ppm Au) have been obtained within the Anomalous Zone where the hanging-wall sericitic zone and the footwall pyritic zone coalesce (Fig. 1).

EXPERIMENTAL PROCEDURES

Samples for the present study were collected from diamond-drill core supplied by LAC Minerals Ltd. Whole-rock trace-element contents were determined by directly coupled plasma spectrometry (DCP) and instrumental neutron activation analysis (INAA) by Neutron Activation Services Ltd., Hamilton, Ontario. Mineral associations were investigated by transmitted- and reflected-light microscopy and electron-microprobe analysis. Chemical compositions of selected mineral grains were analyzed using a JEOL JXA-8600 electron microprobe with Tracor Northern 5500 automation in the Department of Geology at the University of Western Ontario [operation at 25 kV, 20 nA, and beam diameters of 2 to 5 μm, using silicate mineral standards and the synthetic *REE*-bearing calc-silicate glasses of Drake & Weill (1972)]. Matrix corrections were made using the Tracor Northern ZAF program, which accommodates a maximum of only 13 elements per analysis. The 22-element analysis required by this study (Table 1) was made in three separate schedules. Twenty elements were determined in two schedules, with Ca, La, Ce and Nd common to each schedule. Concentrations of Eu and Gd were determined separately in a schedule which included Si, Al, Ca, Fe, La, Ce, Na and P.

Electron-microprobe analysis of *REE* in minerals is not straightforward owing to X-ray line interference (peak overlap; *e.g.*, Exley 1980, Roeder 1985). This interference can be either avoided, by selecting X-ray lines showing minimum interference (Exley 1980), or corrected for, using empirically determined peak-overlap correction factors (Åmli & Griffin 1975). Roeder (1985) analyzed a selection of *REE*-minerals by electron microprobe and found that both methods were satisfactory compared with results of independent chemical analyses. Possible line-interferences and correction factors for wavelength-dispersion spectra are given in Table 2 of Roeder (1985). For the *REE* composition of the present study, the $L\alpha_1$ line of Gd would experience significant interference from Ce$L\gamma_1$. Also the Eu$L\alpha_1$ line would experience minor interference from Nd$L\beta_3$. We avoided these problems by using the $L\beta_1$line for both Gd and Eu; the remaining *REE* (Table 1) were determined with $L\alpha_1$ lines. Owing to the limited amount of sample material and the fine-grained and intimately intergrown nature of unaltered allanite, it was not possible to obtain grain separates for independent determination of *REE* concentrations.

TABLE 1. ELECTRON-MICROPROBE DATA ON ALLANITE, CLINOZOISITE AND MONAZITE

Mineral	allanite		clinozoisite		altered allanite		monazite
	core	mrgn	clz-1	clz-2	core*	mrgn*	mnzt
SiO_2(wt.%)	35.07	33.37	38.25	40.41	34.07	32.66	0.79
TiO_2	0.18	0.15	nd	nd	0.05	0.10	nd
Al_2O_3	23.81	20.60	29.52	31.25	21.06	19.10	0.56
FeO*	5.90	7.93	3.10	1.57	5.15	6.11	0.80
MgO	0.56	1.20	nd	nd	0.61	1.19	0.24
MnO	0.54	1.29	0.30	nd	0.55	1.17	0.02
CaO	17.56	13.12	21.07	24.03	15.12	12.87	0.05
Na_2O	0.20	0.12	nd	nd	0.10	0.15	nd
La_2O_3	2.10	4.48	0.99	nd	1.91	3.75	15.43
Ce_2O_3	4.56	9.00	2.10	nd	4.16	8.64	29.95
Nd_2O_3	2.90	4.15	1.15	nd	2.68	3.91	15.37
Sm_2O_3	0.48	0.56	nd	nd	0.47	0.34	2.72
Eu_2O_3	nd	nd	nd	nd	nd	nd	0.66
Gd_2O_3	0.42	0.51	nd	nd	0.47	0.51	1.77
Dy_2O_3	0.47	0.52	nd	nd	0.45	0.50	1.92
Yb_2O_3	0.05	0.06	nd	nd	0.07	0.05	0.28
Y_2O_3	0.50	0.20	nd	nd	0.89	0.10	0.55
ThO_2	0.20	0.10	nd	nd	0.34	0.20	0.40
U_3O_8	nd	nd	nd	nd	nd	nd	0.13
P_2O_5	nd	nd	nd	nd	nd	nd	28.01
F	0.76	0.50	0.30	nd	0.60	0.45	nd
Cl	0.60	0.86	0.11	nd	0.36	0.60	nd
Total	96.86	98.72	96.81	97.26	89.11	92.40	99.65
O=F,Cl	0.46	0.41	0.15	0.00	0.33	0.32	0.00
Si	3.026	3.030	2.979	3.090			0.031
Ti	0.012	0.010	-----	-----			-----
Al	2.420	2.204	2.774	2.816			0.026
Fe^{2+}	0.343	0.536	0.131	-----			0.034
Fe^{3+}	0.082	0.066	0.076	0.100			-----
Mg	0.073	0.163	-----	-----			0.008
Mn	0.039	0.099	0.020	-----			0.001
ΣM	2.969	3.078	3.001	2.916			
Ca	1.627	1.278	1.805	1.971			0.005
ΣREE	0.343	0.650	0.123	-----			0.964
Th	0.002	0.004	-----	-----			0.003
U	-----	-----	-----	-----			0.001
ΣA	1.972	1.928	1.928	1.971			
P	-----	-----	-----	-----			0.955
F	0.207	0.136	0.074	-----			-----
Cl	0.088	0.126	0.014	-----			-----

* "core" is an average of 10 analyses of REE-poor core of halogen-bearing allanite; "mrgn" is an average of 10 analyses of REE-rich margin; "clz-1" is average of 3 analyses of the REE-bearing clinozoisite nucleus to the REE-poor core; "clz-2" is REE-free clinozoisite inclusion within halogen-bearing allanite. "mnzt" is the average of 3 analyses of monazite associated with halogen-bearing allanite. "FeO*" is total iron; "nd" is not detectable.

Allanite and clinozoisite were calculated on the basis of 12.5 oxygen atoms, and the Fe^{2+}/Fe^{3+} proportions in allanite and REE-bearing clinozoisite were estimated by charge-balance calculation; monazite was calculated on the basis of 4 oxygen atoms.

PETROGRAPHY AND CHEMICAL COMPOSITION

In the study area, epidote-group minerals are ubiquitous in zones of lower metamorphic grade but are typically absent in zones of middle amphibolite facies. Pan & Fleet (1988, 1989a) reported that epidote is one of the most abundant constituents in the cross-cutting calc-silicate veins associated with the late hydrothermal alteration. A chromian epidote (up to 11.8 wt.% Cr_2O_3) associated with zincian chromite has been reported in veins and vesicles in Cr-rich calc-silicate rocks of the Cadi Fracture Zone (Pan & Fleet 1989b, Fig. 1). Allanite of distinct yellowish brown color is restricted to the Anomalous Zone. A typical specimen containing allanite is characterized by abundant sulfides (mainly pyrite, pyrrhotite, chalcopyrite and sphalerite) and calc-silicates (epidote, clinozoisite and prehnite) and a relatively high concentration of gold (up to 27 ppm). Allanite constitutes less than 1 modal %, generally, as fine-grained aggregates, which are closely associated with monazite, apatite, zircon, rutile, tourmaline and clinozoisite, and are surrounded or enveloped by epidote grains (Figs. 2a, b). The majority of allanite aggregates are present in discordance with the main foliation, but a few are also present as elongated micro-boudinages with their long axes parallel or subparallel to the main foliation (Fig. 2b). Locally, allanite crystals of prismatic habit (up to 0.5 x 2 mm) also are present in close association with sulfide veins (Fig. 2c). All of the larger, idioblastic and isolated grains of allanite are altered (*cf.* Ghent 1972). In a few cases, allanite, with other calc-silicate minerals, occurs as inclusions in vein sulfides.

Allanite commonly displays both simple and oscillatory zoning (Bromley 1964, Morin 1977). The simple zoned crystals have been attributed to growth in response to change in fluid composition and to alteration due both to metamictization and leaching (Morin 1977). Unaltered allanite from the White River gold occurrence, with rare exceptions, displays two simple homogeneous zones separated by a distinct boundary. However, the pattern of the compositional zoning is reversed compared to that of common allanite, being characterized by an Al- and Ca-rich, Fe- and *REE*-poor core and an Al- and Ca-poor, Fe- and *REE*-rich margin. In some cases, a third zone also is present as a grain nucleus within the *REE*-poor core (Fig. 2d). The grain nucleus has a composition similar to that of clinozoisite (<3.0 wt.% FeO*) but with a minor content of *REE* (up to 4 wt.% in total REE_2O_3; Table 1). Locally, clinozoisite with about 1.6 wt.% FeO* (total iron) without detectable *REE* also is present as fine inclusions within the grain nucleus (Fig. 2d). This zona-

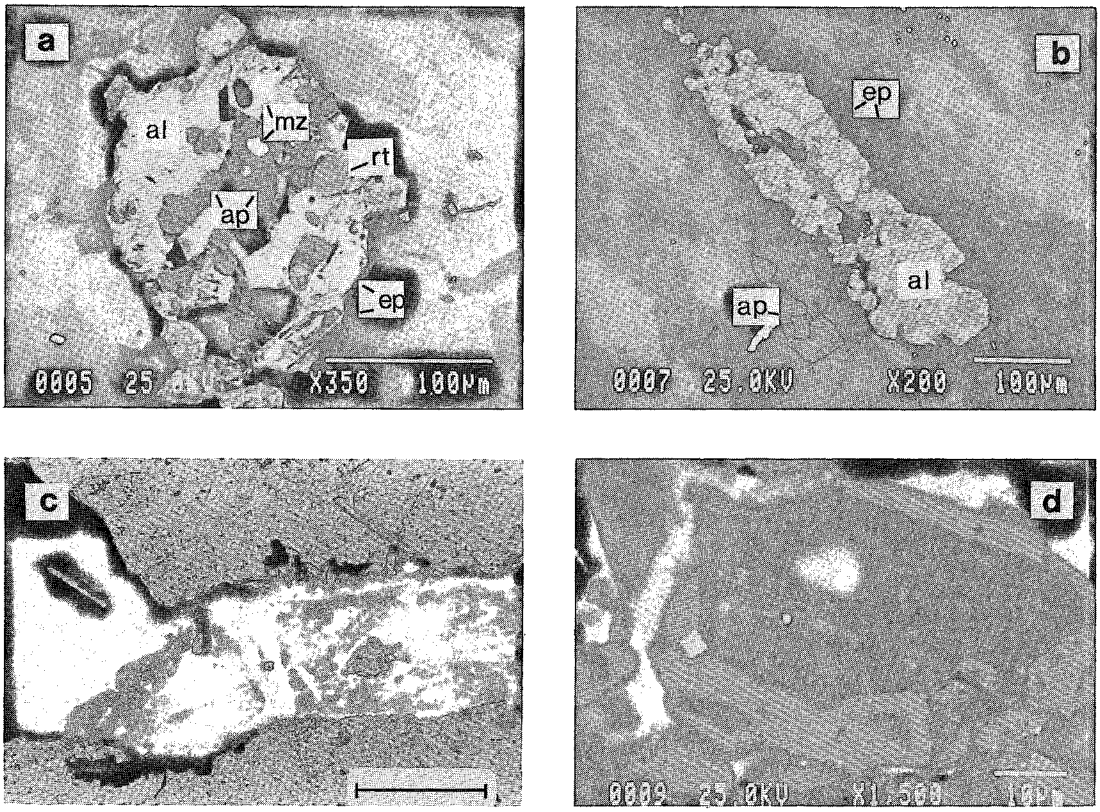

FIG. 2. Halogen-bearing allanite and its textural relationship with associated minerals: (a and b): electron back-scattered images of halogen-bearing allanite aggregates and associated monazite, apatite, rutile, zircon and epidote (al: allanite, mz: monazite, ap: apatite, rt: rutile, ep: epidote); (c) prismatic crystal of allanite associated with vein sulfide (pyrrhotite), scale bar is 0.5 mm; (d) electron back-scattered image of zonal allanite showing *REE*-rich margin (light grey), *REE*-poor core (grey), *REE*-bearing clinozoisite nucleus (dark grey) and *REE*-absent clinozoisite inclusion (dark).

tion of the allanite from the study area appears to be attributable to crystal growth from fluids of changing composition.

Allanite from the study area contains a significant amount of F (up to 0.76 wt.% F) and is characterized by a high chlorine content, which is evident in the energy-dispersion spectrum (EDS). Quantitative electron-microprobe analyses yielded a chlorine content of up to 0.95 wt.% (with average values of 0.86 and 0.60 wt.% Cl in the *REE*-rich margin and the *REE*-poor core, respectively). Therefore, allanite from the study area is a halogen-bearing (F and Cl) variety. Trace amounts of F and Cl also were detected in the grain nucleus (*REE*-bearing clinozoisite, Table 1) within the *REE*-poor core, but typically are absent in the *REE*-free clinozoisite inclusions and in epidote enveloping the grain margin of the halogen-bearing (F and Cl) allanite.

A significant content of medium-sized divalent cations is required in allanite to charge-balance the high content of REE^{3+}. Therefore, allanite is the only member of the epidote group in which ferrous iron is an essential constituent (Deer *et al.* 1986). The halogen-bearing allanite is characteristically lower in total iron content than the summary data listed in Table 7 of Deer *et al.* (1986); based on the charge-balance calculation, nearly all of the iron is inferred to be in the ferrous state. A magnesian allanite (6.2 wt.% MgO) containing less than 2.1 wt.% total Fe as FeO has recently been reported in association with magnesian staurolite and clinozoisite in garnet-corundum rocks from eastern China (Enami & Zang 1988). A plot of ($REE + Fe^{2+} + Mg$) *versus* ($Ca_{A2} + Al_{M3} + Mn$) shows a well-defined linear relationship from clinozoisite to ideal allanite (Fig. 3). Therefore, the concentric zonation in chemical composition from *REE*-free clinozoisite inclusion, passing into *REE*-bearing clinozoisite nucleus, *REE*-poor allanite grain core, to *REE*-rich allanite margin apparently suggests a complete solid-solution between clinozoisite and ideal allanite, represented by the substitution: $Ca_{A2} + Al_{M3} + Mn = REE_{A2} +$

$\mathrm{Fe}^{2+}_{M3}+\mathrm{Mg}$, which can be simplified to $\mathrm{Ca}_{A2}+\mathrm{Al}_{M3}=REE_{A2}+\mathrm{Fe}^{2+}_{M3}$, because Mg and Mn are generally minor and negligible in allanite.

Figure 4 shows the *REE* concentrations of the halogen-bearing allanite from the White River gold occurrence. The chondrite-normalized *REE* patterns of allanite (both core and margin) are characterized by high fractionation between light and heavy *REE*, as indicated by moderate to high $\mathrm{La_N/Yb_N}$ ratios (average 60 and 95 in the core and the margin, respectively). Moreover, the *LREE* (particularly La, Ce, and Nd) are significantly more abundant in the grain margin ($\mathrm{La_{margin}/La_{core}}$ = 2.13, for example), whereas the *HREE* are virtually similar between the grain core and margin.

Other minor constituents, such as Mg and Mn, show slight enrichment in the grain margin relative to the core (0.56 wt.% MgO and 0.54 wt.% MnO in the core, and 1.29 wt.% MgO and 1.20 wt.% MnO in the margin, respectively). Mg and Mn also are present in the grain nucleus (*REE*-bearing clinozoisite) within the core but typically are absent in *REE*-free clinozoisite inclusions and in the epidote surrounding and enveloping grain aggregates of allanite. In contrast to common allanite, Th, U, Sr, and Y are generally low in abundance.

Ghent (1972) noted that allanite decreases in birefringence owing to alteration related to metamictization and weathering. Microprobe analyses on allanite grains of low birefringence (nearly isotropic) yielded oxide totals of 86 to 92 wt.%, somewhat lower than totals for unaltered allanite. Altered allanite also displays chemical zonation and has significantly lower contents of Ca, Fe, Si and Al (and possibly of Cl and F as well) relative to its unaltered counterparts (Table 1), but *REE* contents are not significantly depleted. An unidentified *REE*-rich allanite-like phase was observed in the margin of an altered allanite grain. The single-grain occurrence is about 10 μm in diameter and contains significantly lower Si, Al, Fe and Ca contents than allanite, and P was not detected.

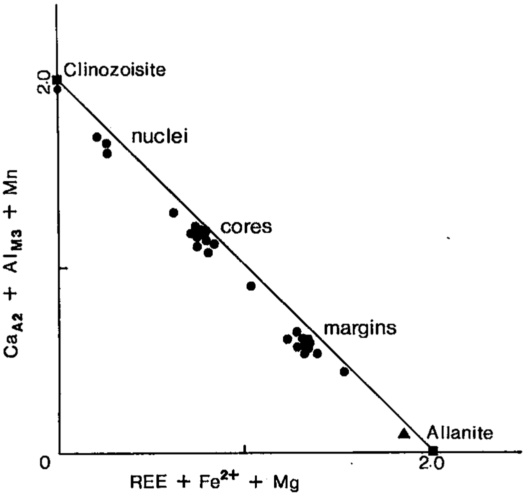

FIG. 3. Clinozoisite–allanite compositions: squares are ideal composition for clinozoisite and allanite end-members; triangle is a Mg-rich allanite from eastern China (Enami & Zang 1988); circles are analytical data from the present study.

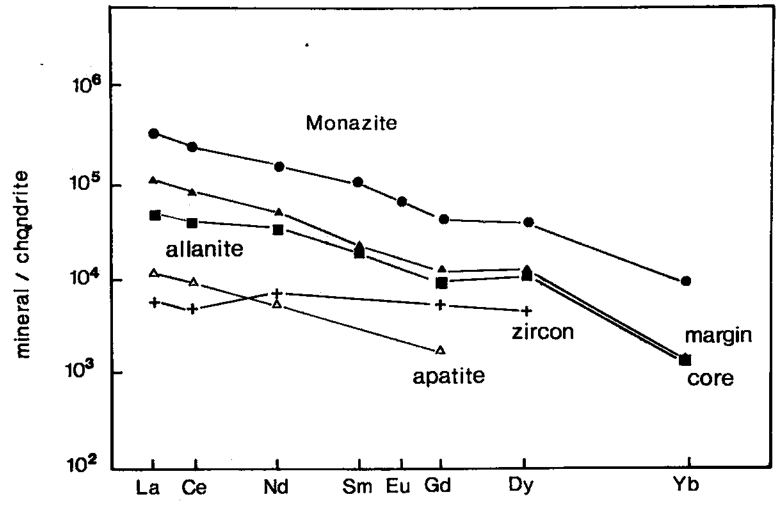

FIG. 4. Chondrite-normalized *REE*-patterns of halogen-bearing allanite, monazite, apatite and zircon: solid circle is monazite; solid square is *REE*-poor core of allanite; solid triangle is *REE*-rich margin of allanite; open triangle is apatite; cross is zircon.

The samples were collected from a few hundred meters below the present surface. Therefore, alteration and leaching are unlikely to be related to weathering. The altered allanite grains commonly contain very fine-grained inclusions of zircon (1 to 2 μm in diameter, or smaller) characterized by 0.5 wt.% ThO_2 and 0.3 wt.% U_3O_8. Therefore, the alteration of the halogen-bearing allanite is probably attributable to metamictization by radioactive elements in zircon. However, alteration due to late-stage hydrothermal fluids cannot be excluded.

DISCUSSION

In the study area, localized calc-silicate alteration is widespread and is exceptionally pervasive within or near major structural failures. It is generally characterized by assemblages consisting of any combination of the following minerals: diopside, grossular (andradite), epidote, prehnite, actinolite, chlorite, clinozoisite, pumpellyite, quartz, microcline, albite, titanite, apatite, and, locally, calcite (Pan & Fleet 1988, 1989a,b). Three calc-silicate occurrences with sulfides (skarns) are of particular interest (Fig. 1); their salient mineralogical and geochemical characteristics strongly correlate with host lithologies. Cr-rich calc-silicates in the Cadi Fracture Zone of the Playter Harbour Group are associated with metamorphosed mafic volcanic rocks and minor ultramafic rocks (Pan & Fleet 1989b). Fe-rich calc-silicates of the Heron Bay Group are associated with metamorphosed high-Fe tholeiitic basalt flows. Thirdly, as presently reported, a *REE*-enriched calc-silicate assemblage is formed in the Anomalous Zone, which is associated with metapelites and metamorphosed intermediate to felsic volcanic rocks.

As described in the previous section, the halogen-bearing allanite in the Anomalous Zone is present invariably within host rocks rather than in veins and generally in direct association with massive epidote or clinozoisite. It is notable that the pistacite contents of *REE*-free clinozoisite inclusions within the core region and epidote forming the outer margin or envelope of the halogen-bearing allanite grain aggregates are similar to their respective massive or vein counterparts. Allanite in skarns (Geijer 1927, 1961, Papunen & Lindsjö 1972) has been found to be characteristically higher in Mg but lower in Th, U, Sr, and Y than some allanite of magmatic origin (Deer *et al.* 1986, Exley 1980, Mitropoulos 1987). The halogen-bearing allanite from the White River gold occurrence has a minor amount of Mg (up to 1.3 wt.% MgO) and also is characterized by low contents in Th, U, Sr and Y. Therefore, the halogen-bearing allanite from the study area is almost certainly part of the calc-silicate (skarn) assemblage.

The high concentrations of Cl and F in allanite from the study area strongly suggest their elevated presence in the ambient hydrothermal fluid. The source of Cl and F (and the hydrothermal fluid itself) is very much an open question, but a few observations on Cl and F are presented here. Detailed microprobe analyses (unpubl. data) reveal that mineral phases of metamorphic assemblages that are parallel to the main foliation at the White River gold occurrence (such as biotite, muscovite and chlorite) contain minor amounts of F but have undetectable amounts of Cl. Apatite associated with allanite aggregates contains Cl as well as F (up to 2.6 wt.% F and 0.5 wt.% Cl), whereas apatite elsewhere in the study area contains up to 3.4 wt.% F, but Cl is not detectable. Furthermore, a trace amount of Cl (up to 0.5 wt.%) and minor F also are detected in some sericite, a common product of late alteration in the Anomalous Zone. Therefore, Cl and F were most likely provided directly by the hydrothermal fluid during alteration. Hornblende, biotite and apatite from the granodioritic Cedar Lake Pluton also contain minor amounts of Cl and F. Therefore, the elevated Cl and F in allanite supports the previous suggestion (Pan & Fleet 1989b) that the hydrothermal fluid responsible for the alteration of the Anomalous Zone could be related directly or indirectly to late plutonic activity.

The unusual reversed *REE* zoning in allanite from the study area (Figs. 2d, 4) is mainly attributable to the *LREE*-enrichment in the grain margin, whereas the *HREE* show no significant variation between the core and margin. Exley (1980) reported "normal" zoning in allanite (*REE*-rich core and *REE*-poor margin) in hydrothermal veins associated with the Skye granites and suggested that the ambient fluid evolved in *REE* chemistry during crystal growth. All of the present allanite grains have a similar (reversed) *REE* zonation, indicating that the ambient fluid evolved to higher La_N/Yb_N values with time. This could be related to variation in the water/rock ratio, permeability, or chemical composition of the hydrothermal fluid itself.

The chondrite-normalized *REE* pattern of monazite also is characterized by high fractionation between *LREE* and *HREE* ($La_N/Yb_N = 35$, Fig. 4, Table 1). Apatite and zircon associated with allanite and monazite in allanite aggregates from the Anomalous Zone also contain considerable amounts of *REE* (up to 7.2 and 4.5 wt.% as REE_2O_3 for apatite and zircon, respectively) and yielded partial *REE* patterns (Fig. 4), whereas *REE* were generally below detection limits of the microprobe in apatite elsewhere in the study area or from the Anomalous Zone but not in association with allanite and monazite. The *REE* pattern of apatite also is similar to those of allanite and monazite and shows *LREE* enrichment over *HREE*. The *REE* composition of zircon is, however, characterized by slight *HREE* enrichment relative to *LREE* (Fig. 4). The similarity

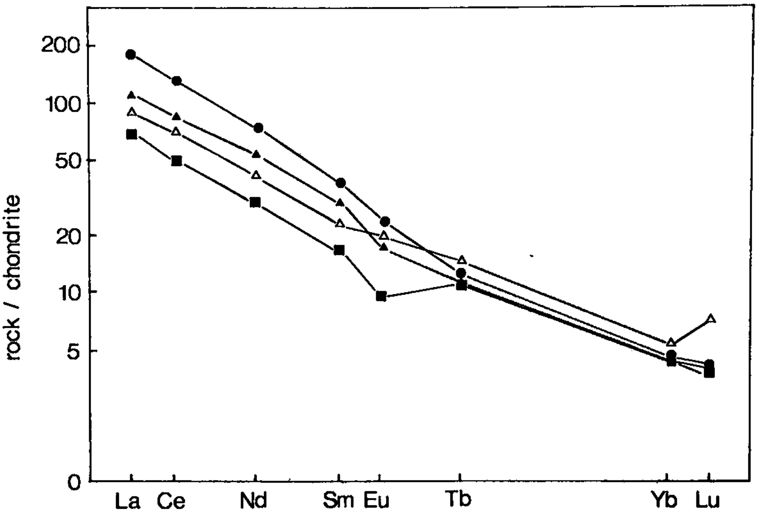

FIG. 5. Chondrite-normalized *REE*-patterns of whole-rock samples from the Anomalous Zone (solid circles represent *REE*-enriched sample, and solid squares represent *REE*-depleted sample), overlying metapelites (solid triangles), and underlying intermediate to felsic metavolcanic rocks (open triangles).

in *REE* patterns of allanite, monazite and apatite suggests that the individual *REE* were partitioned proportionally among these minerals, as in a skarn deposit of Finland (*e.g.*, Fig. 1 of Papunen & Lindsjö 1972), and supports textural evidence that allanite, monazite and apatite crystallized broadly contemporaneously from the hydrothermal fluid. The pattern for zircon is *HREE*-enriched, as expected (zircon is an yttrium-earth mineral, whereas allanite, monazite and apatite are cerium-earth minerals), but it is characteristically flat compared to most patterns of common zircon. This feature suggests that the zircon also was a coexisting phase with other three *REE*-rich minerals, rather than a relict phase, and that its composition reflects the lower mobility of *HREE* relative to *LREE* during hydrothermal alteration (discussed below).

Rare-earth-element behavior during hydrothermal alteration of basaltic materials has been the subject of several studies but remains quite controversial. Hydrothermal experiments (Menzies *et al.* 1979, Hajash 1984) on a glassy tholeiite at temperatures of 150 to 600°C and water/rock ratios of 1 to 125 showed that the *REE* are immobile even where basalt is altered totally to clay. However, other investigators (Staudigel & Hart 1983, Michard *et al.* 1983) suggested that removal (but not fractionation) of *REE* from basalt glass occurs at the basalt–seawater interface where water/rock ratios are extremely high during alteration to palagonite. The present whole-rock data for *REE* (Fig. 5) indicate a wide range of variation for samples from the Anomalous Zone. Most samples are generally similar in both absolute abundances of individual *REE* and chondrite-normalized pattern to the overlying metapelites. However, other samples exhibit selective depletion or addition of *LREE* without significant variation in *HREE*, resulting in change in the fractionation between *LREE* and *HREE*. In a few samples, the total *REE* content is almost doubled, and there is a close correlation between the whole-rock *REE* abundance and modal abundance of allanite and other *REE*-rich minerals. Moreover, the La_N/Yb_N values in the halogen-bearing allanite and monazite are considerably higher than those of whole-rock samples (average of 25, increasing to up to 39 in the halogen-bearing allanite-bearing samples, Fig. 5). Therefore, remobilization of *REE* must have occurred within or in the vicinity of the Anomalous Zone, and mineral stability, particularly of the *REE*-rich minerals, not only affected the *REE* distribution in terms of total *REE* contents but also greatly influenced the *REE* fractionation between *LREE* and *HREE* during hydrothermal alteration. The available evidence suggests that a high water/rock ratio prevailed during calc-silicate alteration in the Anomalous Zone, and elevated contents of F, Cl, and possibly CO_2 must have been present in the hydrothermal fluid, at least for a period of time during alteration, although the hydrothermal fluid was essentially H_2O-rich during calc-silicate alteration, based on a thermodynamic calculation (Pan & Fleet 1989b). Such a fluid could promote the mobility of the *REE* and result in their local concentration (Michard & Albarède 1986, Lottermoser 1989). However, allanite and other *REE*-rich minerals have a very local distribution within the Anomalous Zone, and are found within host rocks rather than in cross-cutting veins. Therefore, we must emphasize that the scale of *REE* mobility was restricted; the *LREE* seem to have been relatively more mobile than the *HREE* during hydrothermal alteration. This finding is consistent with the study of Exley (1980).

Pan & Fleet (1989a) recognized that there is a close correlation between the gold concentration and the abundance of calc-silicate minerals in the Anomalous Zone at the study area. The restricted association of the halogen-bearing allanite and other *REE*-rich minerals within the zone of anomalous gold values further supports a possible genetic link between calc-silicate alteration and gold mineralization in the White River gold occurrence (Pan & Fleet 1989a, 1989b). Calc-silicate minerals also are common in veins at the nearby Hemlo gold deposit, and allanite and monazite also have been reported within its main orebodies (Harris 1986). It is very likely that the calc-silicate alteration, sulfidation and gold mineralization were broadly contemporaneous and related to a complex skarn-like development over a protracted period of time. Secondary sulfides and gold intersecting calc-silicate veins were clearly deposited later in the paragenetic sequence. This Archean auriferous skarn deposit at the White River gold occurrence appears to be analogous to the more familiar Phanerozoic skarn deposits (*e.g.*, Einaudi *et al.* 1981, Einaudi & Burt 1982, Meinert 1984, Brown & Nesbitt 1987). Further discussion on the relationship between skarn development and metallogenesis in the Hemlo - Heron Bay Archean greenstone belt at the Hemlo area will be presented elsewhere.

ACKNOWLEDGEMENTS

We thank LAC Minerals Ltd. for access to the White River property and provision of drill-core materials and geological information. We also thank J. Forth for the preparation of polished thin sections, D.M. Kingston and R.L. Barnett for their assistance with electron-microprobe analyses, N.D. MacRae, S.M. McLennan, and H.W. Nesbitt for discussions on *REE* geochemistry, and two referees for constructive criticism of an earlier manuscript version. The research was supported by an Ontario Geological Survey Grant (No. 305) to MEF.

REFERENCES

ÅMLI, R. & GRIFFIN, W.L. (1975): Microprobe analysis of *REE* minerals using empirical correction factors. *Am. Mineral.* **60**, 599-606.

BROMLEY, A.V. (1964): Allanite in the Tan-Y-Grisiau microgranite, Merionethshire, North Wales. *Am. Mineral.* **49**, 1747-1752.

BROWN, I.J. & NESBITT, B.E. (1987): Gold-copper-bismuth mineralization in hedenbergitic skarns, Tombstone Mountains, Yukon. *Can. J. Earth Sci.* **24**, 2362-2372.

DEER, W.A., HOWIE, R.A. & ZUSSMAN, J. (1986): *Rock-Forming Minerals. 1B. Disilicates and Ring Silicates* (2nd ed.). Longmans, London.

DOLLASE, W.A. (1971): Refinement of the crystal structure of epidote, allanite and hancockite. *Am. Mineral.* **56**, 447-464.

DRAKE, M.J. & WEILL, D.F. (1972): New rare earth element standards for electron microprobe analysis. *Chem. Geol.* **10**, 179-181.

EINAUDI, M.T. & BURT, D.M. (1982): Introduction – terminology, classification, composition of skarn deposits. *Econ. Geol.* **77**, 745-795.

______, MEINERT, L.D. & NEWBERRY, R.J. (1981): Skarn deposits. *Econ. Geol., 75th Anniv. Vol.*, 317-391.

ENAMI, M. & ZANG, Q. (1988): Magnesian staurolite in garnet-corundum rocks and ecologite from the Donghai district, Jiangsu province, east China. *Am. Mineral.* **73**, 48-56.

EXLEY, R.A. (1980): Microprobe studies of *REE*-rich accessory minerals: implications for Skye granite petrogenesis and *REE* mobility in hydrothermal systems. *Earth Planet. Sci. Lett.* **48**, 97-110.

GEIJER, P. (1927): Some mineral associations from the Norberg district. *Sver. Geol. Unders. C.* **343**, 1-32.

______ (1961): The geological significance of the cerium mineral occurrences of the Bastnäs type in central Sweden. *Arkiv Mineral. Geol. Stockholm* **3**, 99-105.

GHENT, E.D. (1972): Electron microprobe study of allanite from the Mt. Falconer quartz monzonite pluton, Lower Taylor Valley, South Victoria Land, Antarctica. *Can. Mineral.* **11**, 526-530.

HAJASH, A., JR. (1984): Rare earth element abundances and distribution patterns in hydrothermal altered basalts: experimental results. *Contrib. Mineral. Petrol.* **85**, 409-412.

HARRIS, D.C. (1986): Mineralogy and geochemistry of the main Hemlo gold deposit, Ontario, Canada. *In* Proc. Gold '86, an International Symposium on the Geology of Gold (Toronto, 1986; A.J. Macdonald, ed.), 297-310.

IVANOV, O.P., VOROB'EV, YU. K., EFREMENKO, L. YA. & KNYAZEVA, D.N. (1981): Acicular allanite from the Itulin deposit veins (further study of lombardite). *Zap. Vses. Mineral. Obshchestva* **110**, 361-366 (in Russ.).

LOTTERMOSER, B.G. (1989): Rare earth element study of exhalites within the Willyama Supergroup, Broken Hill Block, Australia. *Miner. Deposita* **24,** 92-99.

MEINERT, L.D. (1984): Mineralogy and petrology of iron skarns in western British Columbia, Canada. *Econ. Geol.* **79,** 869-882.

MENZIES, M., SEYFRIED, W.E. & BLANCHARD, D. (1979): Experimental evidence of rare earth element immobility in greenstones. *Nature* **282,** 398-399.

MICHARD, A. & ALBARÈDE, F. (1986): The *REE* content of some hydrothermal fluids. *Chem. Geol.* **55,** 51-60.

______, ______, MICHARD, G., MINSTER, J.F. & CHARLOU, J.L. (1983): Rare-earth elements and uranium in high-temperature solutions from East Pacific Rise hydrothermal vein field (13°N). *Nature* **303,** 795-797.

MITROPOULOS, P. (1987): Primary allanite in andesitic rocks from the Poros Volcano, Greece. *Mineral. Mag.* **51,** 601-604.

MORIN, J.A. (1977): Allanite in granitic rocks of the Kenora - Vermilion Bay area, northwestern Ontario. *Can. Mineral.* **15,** 297-302.

MUIR, T.L. (1982): Geology of the Hemlo area, District of Thunder Bay. *Ont. Geol. Surv. Report* **218.**

PAN, Y. & FLEET, M.E. (1988): Metamorphic petrology of the White River gold prospect, Hemlo area, Ontario. *Ont. Geol. Surv. Misc. Pap.* **140,** 165-176.

______ & ______ (1989a): Metamorphic petrology and gold mineralization of the White River gold prospect, Hemlo area, Ontario. *Ont. Geol. Surv. Misc. Pap.* **143,** 42-52.

______ & ______ (1989b): Cr-rich calc-silicates from the Hemlo area, Ontario. *Can. Mineral.* **27,** 565-577.

PAPUNEN, H. & LINDSJÖ, O. (1972): Apatite, monazite and allanite, three rare-earth minerals from Korsnäs, Finland. *Geol. Soc. Finland Bull.* **44,** 123-129.

RAO, A.T., RAO, A. & RAO, P.P. (1979): Fluorian allanite from calc-granulite and pegmatite contacts at Garvidi, Andhra Pradesh, India. *Mineral. Mag.* **43,** 312.

ROEDER, P.L. (1985): Electron-microprobe analysis of minerals for rare-earth elements: use of calculated peak-overlap corrections. *Can. Mineral.* **23,** 263-271.

STAUDIGEL, H. & HART, S.R. (1983): Alteration of basalt glass: mechanism and significance for the oceanic crust - seawater budget. *Geochim. Cosmochim. Acta* **47,** 337-350.

Received July 17, 1989, revised manuscript accepted December 5, 1989.